

This item is the archived peer-reviewed author-version of:

Radical oxidation of methyl vinyl ketone and methacrolein in aqueous droplets : characterization of organosulfates and atmospheric implications

Reference:

Wach Paulina, Spolnik Grzegorz, Rudzinski Krzysztof J., Skotak Krzysztof, Claeys Magda, Danikiewicz Witold, Szmigielski Rafal.- Radical oxidation of methyl vinyl ketone and methacrolein in aqueous droplets : characterization of organosulfates and atmospheric implications
Chemosphere - ISSN 0045-6535 - 214(2019), p. 1-9
Full text (Publisher's DOI): <https://doi.org/10.1016/J.CHEMOSPHERE.2018.09.026>
To cite this reference: <https://hdl.handle.net/10067/1553650151162165141>

Accepted Manuscript

Radical oxidation of methyl vinyl ketone and methacrolein in aqueous droplets:
characterization of organosulfates and atmospheric implications

Paulina Wach, Grzegorz Spólnik, Krzysztof J. Rudziński, Krzysztof Skotak, Magda
Claeys, Witold Danikiewicz, Rafał Szmigielski



PII: S0045-6535(18)31679-5

DOI: 10.1016/j.chemosphere.2018.09.026

Reference: CHEM 22106

To appear in: *Chemosphere*

Received Date: 21 June 2018

Accepted Date: 04 September 2018

Please cite this article as: Paulina Wach, Grzegorz Spólnik, Krzysztof J. Rudziński, Krzysztof Skotak, Magda Claeys, Witold Danikiewicz, Rafał Szmigielski, Radical oxidation of methyl vinyl ketone and methacrolein in aqueous droplets: characterization of organosulfates and atmospheric implications, *Chemosphere* (2018), doi: 10.1016/j.chemosphere.2018.09.026

This is a PDF file of an unedited manuscript that has been accepted for publication. As a service to our customers we are providing this early version of the manuscript. The manuscript will undergo copyediting, typesetting, and review of the resulting proof before it is published in its final form. Please note that during the production process errors may be discovered which could affect the content, and all legal disclaimers that apply to the journal pertain.

1 **Radical oxidation of methyl vinyl ketone and methacrolein in aqueous droplets:**
2 **characterization of organosulfates and atmospheric implications**

3

4 Paulina Wach ^{a)*}, Grzegorz Spólnik ^{b)}, Krzysztof J. Rudziński ^{a)}, Krzysztof Skotak^{c)}, Magda
5 Claeys ^{d)}, Witold Danikiewicz ^{b)} and Rafał Szmigielski ^{a)*}

6

7 ^{a)} Institute of Physical Chemistry, Polish Academy of Sciences, ul. Kasprzaka 44/52, 01-224
8 Warsaw, Poland

9 ^{b)} Institute of Organic Chemistry, Polish Academy of Sciences, ul. Kasprzaka 44/52, 01-224
10 Warsaw, Poland

11 ^{c)} Institute of Environmental Protection-National Research Institute, ul. Krucza 5/11D, 00-548
12 Warszawa, Poland

13 ^{d)} Department of Pharmaceutical Sciences, University of Antwerp, BE 2610 Antwerp, Belgium

14

15 *Corresponding author:

16 Phone: +48 (22) 343 3402, e-mail: ralf@ichf.edu.pl pwach@ichf.edu.pl

17

18

19

20

21

22

23

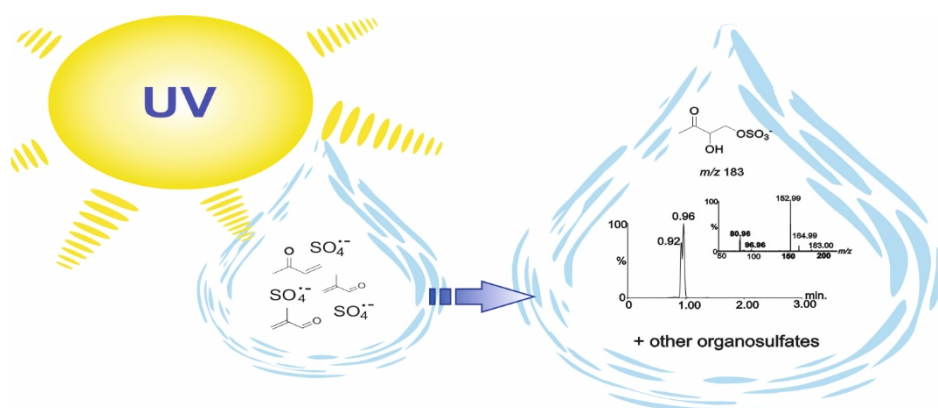
24

25

26

27

28

29 **Graphical Abstract**

30

31

32 **Abstract**

33

34 In-cloud processing of volatile organic compounds is one of the significant routes leading to
 35 secondary organic aerosol (SOA) in the lower troposphere. In this study, we demonstrate
 36 that two atmospherically relevant α,β -unsaturated carbonyls, i.e., but-3-en-2-on (methyl vinyl
 37 ketone, MVK) and 2-methylpropenal (methacrolein, MACR), undergo sulfate radical-
 38 induced transformations in dilute aqueous systems under photochemical conditions to form
 39 organosulfates previously identified in ambient aerosols and SOA generated in smog
 40 chambers. The photooxidation was performed under sun irradiation in unbuffered aqueous
 41 solutions containing carbonyl precursors at a concentration of 0.2 mmol and peroxydisulfate
 42 as a source of sulfate radicals ($\text{SO}_4^{\bullet-}$) at a concentration of 0.95 mmol. UV-vis analysis of
 43 solutions showed the fast decay of unsaturated carbonyl precursors in the presence of
 44 sulfate radicals. The observation confirms the capacity of sulfate radicals to transform the
 45 organic compounds into SOA components in atmospheric waters. Detailed interpretation of
 46 high-resolution negative ion electrospray ionization tandem mass spectra allowed to assign
 47 molecular structures to multiple aqueous organosulfate products, including an abundant
 48 isoprene-derived organosulfate $\text{C}_4\text{H}_8\text{SO}_7$ detected at m/z 199. The results highlight the solar
 49 aqueous-phase reactions as a potentially significant route for biogenic SOA production in
 50 clouds at locations where isoprene oxidation occurs. A recent modelling study suggests that

51 such processes could likely contribute to 20-30 Tg year⁻¹ production of SOA, referred to as
52 aqSOA, which is a non-negligible addition to the still underestimated budget of atmospheric
53 aerosol.

54

55 **Highlights**

56

- 57 • Methacrolein and methyl vinyl ketone form SOA in atmospheric waters
- 58 • This proceeds through SO₄ radical-mediated reactions to form organosulfates
- 59 • Structures of organosulfates formed were elucidated and in some cases revised
- 60 • An abundant isoprene-related organosulfate C₄H₈SO₇ (*m/z* 199) was detected
- 61 • Sunlight enhances the oxidative capacity of atmospheric waters

62

63 **Keywords**

64

65 secondary organic aerosol, aqueous photochemistry, organosulfates, sulfate radicals, methyl
66 vinyl ketone, methacrolein

67

68

69

70

71

72

73

74

75

76

77

78

79 1. Introduction

80

81 Secondary organic aerosol (SOA) produced in the troposphere receives considerable
82 attention for several reasons. First, it affects human life and health by triggering various lung
83 and cardiovascular diseases. Second, it decreases visibility and destroys architectural
84 monuments. Third, it impacts the Earth's climate through scattering and absorbing solar
85 radiation and acting as cloud condensation nuclei (Bianchi et al., 2016).

86 Despite intensive laboratory and modelling studies, and field measurements with
87 advanced analytical instrumentation and modelling, our understanding of the formation and
88 growth of aerosol particles is still highly constrained (Hallquist et al., 2009; Nozière et al.,
89 2015; Zhao et al., 2017).

90 The formation of SOA components from trace gases is fairly well characterized in
91 respect to the most abundantly released biogenic hydrocarbons, including isoprene
92 (2-methylbuta-1,3-dien, ISO), terpenes and sesquiterpenes. Isoprene is a key precursor of
93 ambient SOA because of its emission rate which is highest of all non-methane hydrocarbons
94 (Sindelarova et al., 2014) and its high reactivity due to two conjugated double bonds. In
95 addition to SOA formation via gas-phase photooxidation of volatile precursors followed by
96 gas-to-particle partitioning of its semi-volatile oxidation products and heterogeneous particle-
97 bound processes (Hallquist et al., 2009), aqueous-phase organic reactions have been
98 recently suggested to contribute to SOA (aqSOA). Yet, over the last few years another type
99 of mechanism has been intensively investigated – atmospheric reactions occurring in
100 aqueous media (Claeys et al., 2004; Rudziński et al., 2009; Liu et al., 2012; Schone et al.,
101 2014; Szmigielski, 2016; Giorio et al., 2017). Aqueous-phase reactions of ISO and its gas-
102 phase oxidation products, such as methyl vinyl ketone (MVK) or methacrolein (MACR), have
103 been proposed as alternative routes to SOA formation. These include reactions taking place
104 on the surface of water droplets or in the bulk of water solutions (Blando and Turpin, 2000;
105 Kameel et al., 2014; Nozière, 2016; Szmigielski, 2016). So far, the role of MVK and MACR in
106 these reactions has been largely neglected because of their low solubility in water (Henry

107 coefficients: $H_{\text{MACR}} = 6.5 \text{ mol atm}^{-1}$ and $H_{\text{MVK}} = 41 \text{ mol atm}^{-1}$) (Leng et al., 2013). However,
108 recent reports showed that both compounds are found in the aqueous phase at much higher
109 concentrations than predicted from their Henry's coefficients (Schöne and Herrmann, 2014;
110 Herrmann et al., 2015; McNeill, 2015). The concentrations of MACR and MVK measured in
111 atmospheric waters ranged from $0.01 - 0.5 \times 10^{-3} \text{ mmol L}^{-1}$ and $0.05 - 2.2 \times 10^{-3} \text{ mmol L}^{-1}$,
112 respectively (Van Pinxteren et al., 2005). Estimated global production of biogenic SOA in
113 cloud water reaches 20-40 Tg year⁻¹, including the contribution from cloud processing of ISO
114 and MVK as high as 2-3 Tg year⁻¹ (McNeill, 2015). "Other carbonyls originating from
115 isoprene, including glyoxal, methylglyoxal, 2-methylglyceric acid and hydroxyacetone, also
116 contribute to the organic aerosol mass through in-cloud processes" (Carlton et al., 2009;
117 Ervens et al., 2011; Noziere, 2016). These processes are predominantly controlled by OH
118 radicals, which are ubiquitous in the lower atmosphere (Monks, 2005). However,
119 atmospheric water droplets can perfectly house reaction systems governed by other radical
120 species (Herrmann et al., 2015). Of these, the sulfate radical anion ($\text{SO}_4^{\bullet -}$) plays an ample
121 role since it has a great oxidation capacity (Ouyang et al., 2005) and the propensity to add to
122 unsaturated olefins (Rudzinski, 2004; Rudziński et al., 2009; Liang et al., 2016).

123 Our previous studies (Rudzinski, 2004; Rudziński et al., 2009; Schöne and Herrmann,
124 2014; Rudzinski et al., 2016) along with reports from other laboratories (Nozière et al., 2010;
125 Schindelka et al., 2013; Shalamzari et al., 2016) showed that the sulfate radical anions are a
126 powerful driver for aqueous processing of isoprene and C₄-C₅ carbonyls leading to a series of
127 organosulfates, which are relevant markers of the polar SOA fraction. In this study we
128 focused on the molecular composition of aqSOA formed via sunlight-induced aqueous
129 photochemistry of two water-soluble α,β -unsaturated carbonyls, i.e., MVK and MACR – as
130 main products of isoprene oxidation in the atmosphere and potassium persulfate – as a
131 simple precursor of aqueous sulfate radicals.

132 The experimental setup was intended to mimic natural atmospheric conditions as
133 much as possible with a natural source of UV-vis wavelengths provided by sunlight and with

134 the use of diluted solutions of organic and inorganic species. To the best of our knowledge,
135 such an approach has never been applied before. A key point of the study was to obtain
136 insights into the chemistry taking place in the bulk aqueous phase in respect to the formation
137 of SOA organosulfates. The progress of the aqueous-phase reactions of selected carbonyls
138 with the sulfate radical anion was followed by UV-vis spectroscopy. Small molecular weight
139 (MW) products were structurally characterized using ultra-high performance liquid
140 chromatography combined with high resolution tandem mass spectrometry. The chemical
141 composition of aqSOA samples obtained from laboratory experiments was compared with
142 Diabla Gora ambient PM_{2.5} (particles with diameters lower than 2.5 µm aerodynamic
143 diameter) aerosol collected during the 2014 summer campaign in the north-eastern rural
144 region in Poland (Masuria Province). This region is dominated by broad-leaf forests providing
145 a local source of isoprene and isoprene-related oxidized volatile organic compounds,
146 including MACR and MVK.

147

148 **2. Materials and methods**

149

150 *2.1. Chemicals*

151

152 High-purity water (18.2 MΩ·cm resistivity at 25 °C) used for the aqueous-phase experiments,
153 reconstitution of aerosol extracts and preparation the LC mobile phase was obtained using a
154 Milli-Q Advantage water purification system (Merck, Darmstadt, Germany). The following
155 chemicals were used for the reactions without further purification: potassium persulfate,
156 K₂S₂O₈, (pure, POCH, Poland), methyl vinyl ketone (99 %; Sigma Aldrich, St. Louis, MO
157 63103, USA), methacrolein (95 %; Sigma Aldrich). All solutions were prepared freshly before
158 each experimental run.

159

160 *2.2. Aqueous-phase*

161

162 A series of sunlight-induced aqueous-phase experiments were performed using stock
163 solutions of oxidized isoprene C₄ derivatives, i.e., methyl vinyl ketone (MVK) and
164 methacrolein (MACR). Concentrations of carbonyl compounds were 0.19 mmol L⁻¹, while the
165 inorganic potassium persulfate (K₂S₂O₈), the sulfate radical precursor (Kolthoff, 1951; C. von
166 Sonntag, 1991), was 0.16 mmol L⁻¹. Reactions were conducted in the 1 mL quartz cuvettes,
167 exposed to sun irradiation for 200 min during a summer day. All
168 the experimental parameters, such as the decay of organic reactant, the ambient air
169 temperature, and the light intensity were controlled every 30 min. The temperature of
170 ambient air in close vicinity of the reaction vessels ranged from 298 to 303 K, while the
171 sunlight intensity measured with an ILT 1400A radiometer (International Light Technologies)
172 varied from 26.8 to 33.1 mW cm². UV-vis spectra were recorded with a Jasco V-570
173 spectrophotometer within the range of 200-300 nm (band width 0.1 nm, data pitch: 0.5 nm,
174 scanning speed: 400 nm min⁻¹). As a baseline reference, Milli-Q water was used. The
175 reference spectra for MAC and MVK were acquired with the same concentration levels, i.e.,
176 0.19 mmol L⁻¹, and measurement parameters as stated above.

177 For comparison, dark experiments were performed following the same procedures as those
178 for the runs. Stock solutions of carbonyl compounds and potassium persulfate were freshly
179 prepared before each experiment and stored wrapped in aluminium foil. The UV-vis and
180 negative ion electrospray mass spectra of aliquots were recorded immediately after
181 sampling. Samples used for the mass spectral analyses were diluted with methanol (1:1;
182 v/v).

183 184 2.3. *Aerosol samples*

185
186 Ambient PM_{2.5} aerosol samples were collected in 24 hour periods during the summer
187 campaign (July 26-31, 2014) in Diabla Gora, Poland, on 15 cm quartz fibre filters using a
188 high-volume aerosol sampler (Digitel DHA-80, Switzerland). Diabla Gora is located in a rural
189 site in the Borecka forest of the Masuria Province (54°07'29.52"N; 22°02'17.08"E).

190 The sampling site is surrounded by lakes and dense broad-leaf forest stands providing
191 an important local source for isoprene emission and formation of isoprene-derived carbonyls.
192 The Diabla Gora station is a reference station for measuring clean air masses and monitoring
193 air pollution according to the European Monitoring Evaluation Policy. After sample collection,
194 filters were wrapped in a prebaked aluminum foil and stored at $-20\text{ }^{\circ}\text{C}$ until further analysis.
195 The filter extracts were prepared as follows: two 1 cm^2 punches were cut from each selected
196 quartz fibre filter and were extracted 3 times with 10 mL of methanol using a PSU-20i orbital
197 shaker (Biosan, Poland) for 10 min. The extracts were combined and concentrated to 1 mL
198 using a Büchi rotary evaporator ($35\text{ }^{\circ}\text{C}$, reduced pressure), filtered through a $0.2\text{ }\mu\text{m}$ Teflon
199 filter, and evaporated to dryness with a gentle stream of nitrogen. The obtained dry residues
200 were reconstituted in $140\text{ }\mu\text{L}$ of methanol/water (1:1; v/v) and used for further analyses.

201

202 2.4. *High resolution LC/MS analysis*

203

204 Products of aqueous-phase reactions and extracts of ambient $\text{PM}_{2.5}$ aerosol were screened
205 using a high resolution Synapt G2-S HDMS (Waters, Poland) mass spectrometer. The
206 instrument was equipped with an electrospray ion source and a quadrupole – time-of-flight
207 mass analyzer. Measurements were carried out in the negative ion mode with a sampling
208 cone voltage of 20 V, a capillary voltage of 3 kV and a FWHM (full-width-at-half-maximum)
209 mass resolving power of 20 000. The MS unit was coupled with a Waters UHPLC ACQUITY
210 UPLC I-Class system (Waters, Poland), equipped with an ACQUITY UPLC HSS T3 column
211 ($1.8\text{ }\mu\text{m}$, $2.1\text{ x }100\text{ mm}$). The applied mobile phases consisted of 20 mmol ammonium
212 acetate (A) and methanol (B). The gradient elution program was as follows: the concentration
213 of eluent A was kept at 100% for the first 3 min with a flow rate 0.35 mL/min . During the next
214 5 min eluent B was increased to 100% and was kept at this level for 2 min. For the last 3 min
215 eluent B was decreased to 0%. The data processing and the instrument control were done
216 using a MassLynx V4.1 software package (Waters, Poland).

217

218

219 3. Results and discussion

220

221 3.1. Formation of organosulfates

222

223 Based on 2009 (Hallquist et al., 2009), 2011 (Ervens et al., 2011) and 2015 (Nozière et al.,
224 2015) review papers, aqSOA samples containing organosulfates can be produced in a
225 laboratory framework through in-cloud chemistry under dark and/or solar conditions. In the
226 dark mode two atmospherically relevant pathways have been suggested: (1) addition of the
227 sulfate radicals onto an unsaturated C=C bond of the precursor (Szmigielski, 2016; Kwong et
228 al., 2018), (2) nucleophilic addition of the sulfate anion onto an isoprene-derived epoxy ring
229 (Darer et al., 2011; Nguyen et al., 2014). In contrast, solar approaches have entailed (1) UV
230 irradiation of concentrated solutions of ammonium sulfate and the organic precursor (Nozière
231 et al., 2010), (2) laser photolysis of concentrated solutions containing sulfate peroxide and
232 carbonyl precursors (Schindelka et al., 2013). In either case radicals formed (e.g., OH, SO₄)
233 add onto biogenic olefins to spur further transformations. We have decided to perform the
234 solar experiment as close to the natural environment as possible, by using sun irradiation to
235 generate sulfate radicals in diluted solutions of organic precursors. In case of both selected
236 precursors, our mimicking experiments revealed the formation of a variety of products,
237 including atmospherically-relevant organosulfates.

238

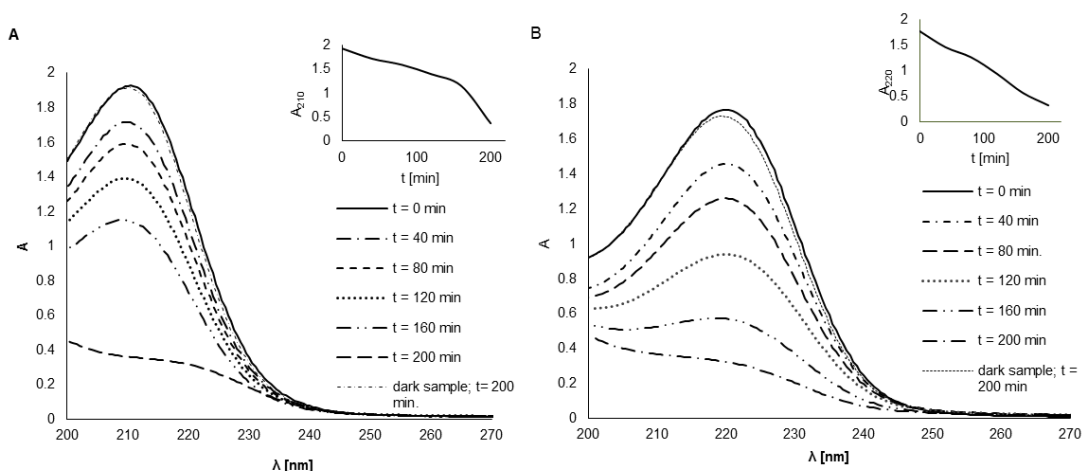
239 3.2. UV-vis observations of MVK and MACR decay

240 The decay of organic compounds (MVK, MACR) during each experiment, were monitored
241 using UV-vis spectroscopy. The results obtained under irradiation were compared with those
242 recorded for dark conditions to exclude any chemical artefacts. For methyl vinyl ketone and
243 methacrolein the maxima of absorption were measured in a shortwave UV range – intense
244 absorption bands are located at the wavelengths of ca. 210 nm (MVK), and ca. 220 nm

245 (MACR), respectively, which correspond to the $\pi \rightarrow \pi^*$ transition. The presence of these
 246 bands suggest the existence of MACR and MVK in their carbonyl forms in aqueous solutions,
 247 which are in line with an earlier study (Renard et al., 2015).

248 The irreversible loss of MVK and MACR during the photooxidation experiment (Fig.1)
 249 suggests the occurrence of chemical processes leading to an array of novel products.

250



251

252 **Fig.1** Decay of UV absorption bands for A) methyl vinyl ketone (λ_{\max} 210 nm) and B)
 253 methacrolein (λ_{\max} 220 nm) during the aqueous-phase reaction with sulfate radicals
 254 (experimental conditions: mean temperature 300 K, mean light intensity 31.5 mW cm²).
 255 Insets show maxima of the absorption bands in function of time.

256

257 We can observe that the UV spectra of the first sample ($t = 0$ min) after the addition of
 258 potassium persulfate (before exposure to sun light) and for the dark sample (dark sample; $t =$
 259 200 min) are comparable within an experimental measurement. When exposed to sun
 260 irradiation, there is a gradual loss of absorption until a reaction time of 160 min, after which
 261 we can observe the greatest loss of absorption band for MVK. After 200 min of sun exposure
 262 MVK is completely consumed. The difference between the sun-irradiated sample and that
 263 kept in a dark environment is obvious, indicating that natural occurring UV light significantly

264 accelerates the decrease of organic precursor due to the effective radical formation *via*
265 photolysis.

266 A similar situation was obtained for aqueous photooxidation of methacrolein in the
267 presence of potassium persulfate (Fig. 1 B), where after 200 min reaction time a difference
268 between the sun-irradiated sample and the dark one is clearly observable – most of the olefin
269 is consumed considering the intensity of absorption band for unreacted MACR. In contrast to
270 MVK, methacrolein was consumed evenly during the reaction.

271

272 3.4. Chemical characterization of products from aqueous photooxidation of MVK

273

274 The analyses of organosulfates formed during the irradiation of the aqueous solution
275 containing methyl vinyl ketone and potassium persulfate were targeted to low-MW C₃-C₄
276 products. The mass spectrometric data for detected organosulfates in both aqueous-phase
277 reactions and ambient PM_{2.5} extracts along with suggested structures are summarized in
278 Table 1. All of the listed organosulfates were reported in the literature as products of
279 reactions conducted with use of different modes of sulfate radicals formation (Nozière et al.,
280 2010; Schindelka et al., 2013).

281 Table 1. Detected organosulfates from aqueous SOA and ambient $PM_{2.5}$ extracts along with their proposed structures.

Organic precursor	[M – H] ⁻	Error [mDa]	Formula	No. of isomers	Aqueous-phase reaction	Ambient sample	Suggested structure
MVK	152.9859	+ 0.1	C ₃ H ₅ O ₅ S	1	present	present	
MVK	154.9652	+ 0.2	C ₂ H ₃ O ₆ S	1	present	present	
MVK	167.0018	+ 0.4	C ₄ H ₇ O ₅ S	1	present	not	
MVK	182.9958	- 0.5	C ₄ H ₇ O ₆ S	2	present	one isomer is present (on the left)	
MVK	198.9911	- 0.1	C ₄ H ₇ O ₇ S	1	present	not	
MACR	152.9857	-0.1	C ₃ H ₅ O ₅ S	1	present	present	
MACR	182.9962	-0.1	C ₄ H ₇ O ₆ S	1	present	not	
MACR	198.9939	+1.5	C ₄ H ₇ O ₇ S	1	present	present	

283 *MW 154, 156 and 168 organosulfates*

284

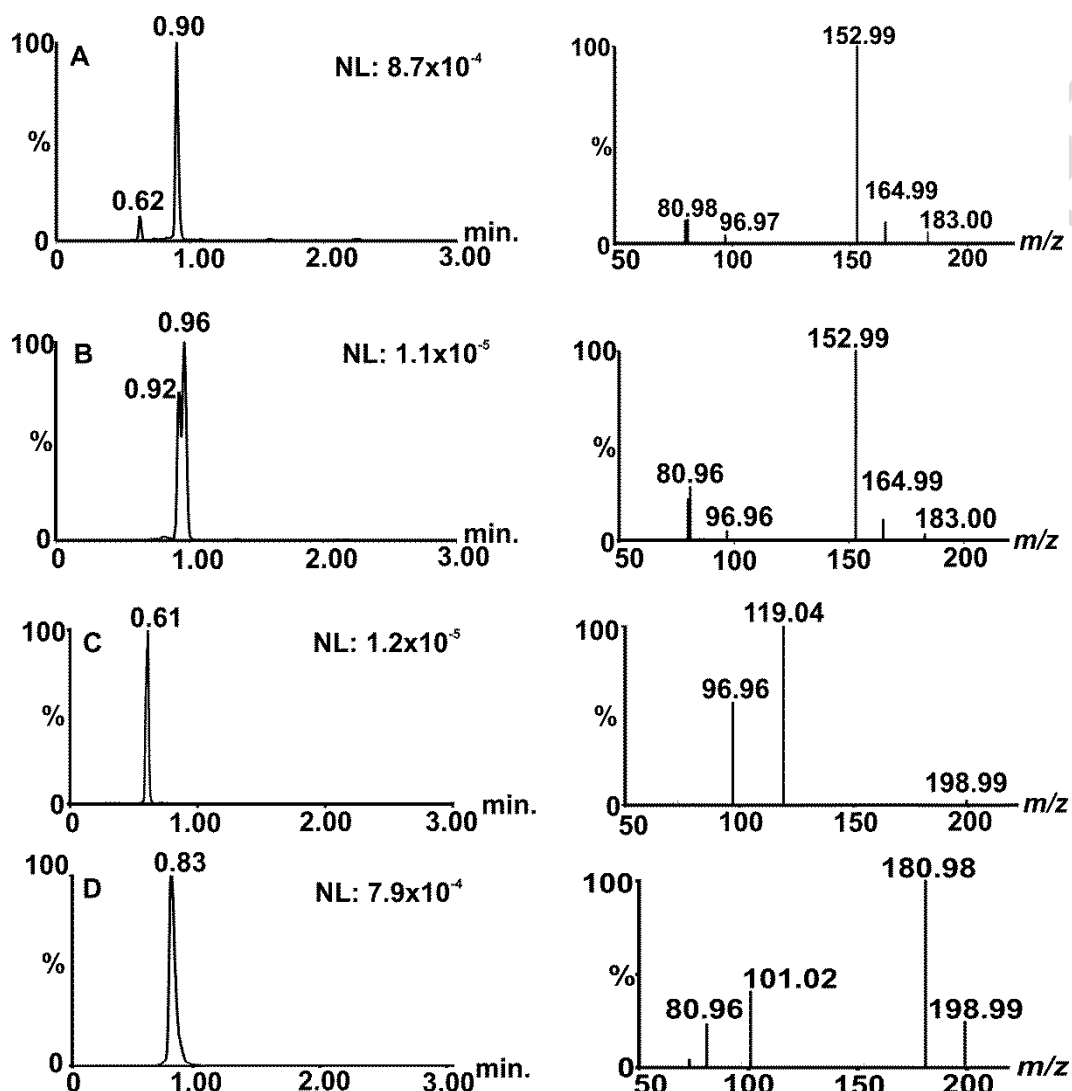
285 The MW 154 organosulfate detected in both PM_{2.5} ambient aerosol and aqSOA from MVK
286 appeared as a single peak in the chromatographic analysis, which indicates the simple
287 molecular structure of hydroxyacetone sulfate. Our finding is in line with earlier reports from
288 ambient and laboratory experiments and could be rationalized by the SO₄ radical addition to
289 the MVK unsaturated bond (Safi Shalamzari et al., 2013; Schindelka et al., 2013). The
290 appearance of the MW 156 organosulfate in ambient PM_{2.5} aerosol and in the aqueous-
291 phase experiment as a single chromatographic peak points to a further oxidation product. For
292 MW 156 organosulfate the structure of sulfated glycolic acid (Table 1) is suggested, which is
293 likely formed *via* the reactive uptake of glyoxal on ammonium sulfate seed aerosol under
294 irradiated conditions (Safi Shalamzari et al., 2013). However, the underlying photochemical
295 mechanism is not clear. Here, we propose that the MW 156 organosulfate forms from MVK
296 as a result of the addition of the hydroxyl radical to the earlier-formed hydroxyacetone sulfate
297 in the aqueous-phase. In the case of the MW 168 organosulfate the results obtained are
298 different – although such a product is formed during the reaction; however, its retention time
299 does not correspond to the MW 168 organosulfate reported elsewhere for PM_{2.5} ambient
300 samples (Schindelka et al., 2013), suggesting the MVK reaction channel has no significance
301 towards its formation in the atmosphere. However, the MW 168 organosulfate has recently
302 been reported in Arctic aerosol (Hansen et al., 2014) and suggested by earlier studies to
303 originate from methacrolein based on smog chamber measurements of the photochemical
304 oxidation of isoprene in the presence of acidic sulfate aerosol (Surratt et al., 2007;
305 Szmigielski et al., 2007).

306 *MW 184 organosulfate*

307

308 During the irradiation of MVK solutions we could observe the appearance of two isomeric
309 products, which elute from the LC column at 0.92 and 0.96 min, respectively (Fig. 2 B).

310 Accurate mass measurements allowed the assignment of these products as the MVK-related
 311 organosulfate with the MW 184 ($C_4H_7O_6S$; measured mass: 182.9965; error: 0.2 mDa).
 312

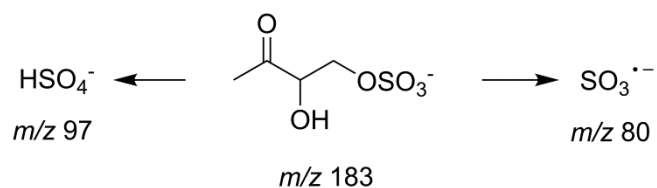


313
 314
 315 **Fig. 2.** Extracted ion chromatograms along with negative ion electrospray product ion spectra
 316 recorded for: A) m/z 183 ion in the fine ambient $PM_{2.5}$ aerosol sample; B) m/z 183 ion in the
 317 MVK aqueous sample (the product ion spectrum for the RT 0.92 min isomer is not shown);
 318 C) m/z 199 ion in the ambient $PM_{2.5}$ aerosol sample; D) m/z 199 ion in the MVK aqueous
 319 sample.

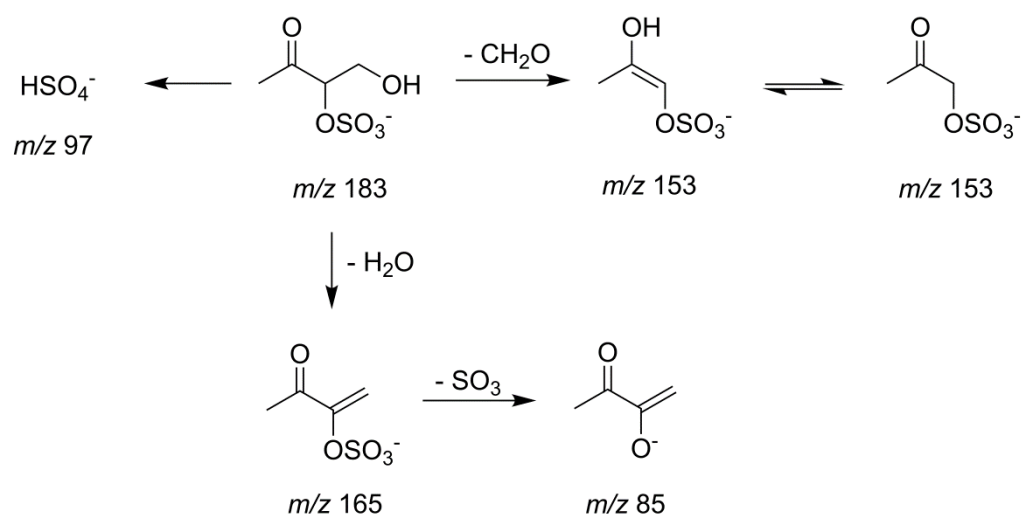
320

321 The presence of the two weakly resolved peaks in the chromatographic profile points to
322 positional isomers, which could differ by the position of the sulfate group in the molecule.
323 Although the MW 184 organosulfate has been reported in earlier studies (Surratt et al., 2006;
324 Schindelka et al., 2013; Shalamzari et al., 2016), the separation and structural differentiation
325 of its isomers failed due to a poor chromatographic resolution. The m/z 183 product ion mass
326 spectrum recorded for the major RT 0.96 min isomer revealed a m/z 183 \rightarrow m/z 153
327 transition, corresponding to the neutral loss of CH_2O (formaldehyde), which points to the
328 presence of a terminal primary OH group (Scheme 1 B2). Interestingly, the same
329 fragmentation behavior was not evidenced for the RT 0.92 min isomer (spectra not shown),
330 which suggests the presence of a sulfated primary OH group and a secondary OH group in
331 the MVK-retained backbone (Scheme 1 B1). A detailed discussion of the issue was reported
332 elsewhere (Safi Shalamzari et al., 2013; Szmigielski, 2016; Spolnik et al., 2018). The
333 comparison of LC-MS data for ambient $\text{PM}_{2.5}$ aerosol and laboratory-generated aqSOA
334 revealed that the later-eluting isomer (RT 0.96 min) of the MW 184 organosulfate produced
335 from the laboratory experiment is present in ambient $\text{PM}_{2.5}$ aerosol (RT 0.90 min) as
336 indicated by its chromatographic and mass spectral properties. The reason for the difference
337 in the retention times could be in very different chemical composition of matrices in the two
338 samples.
339

B1



B2



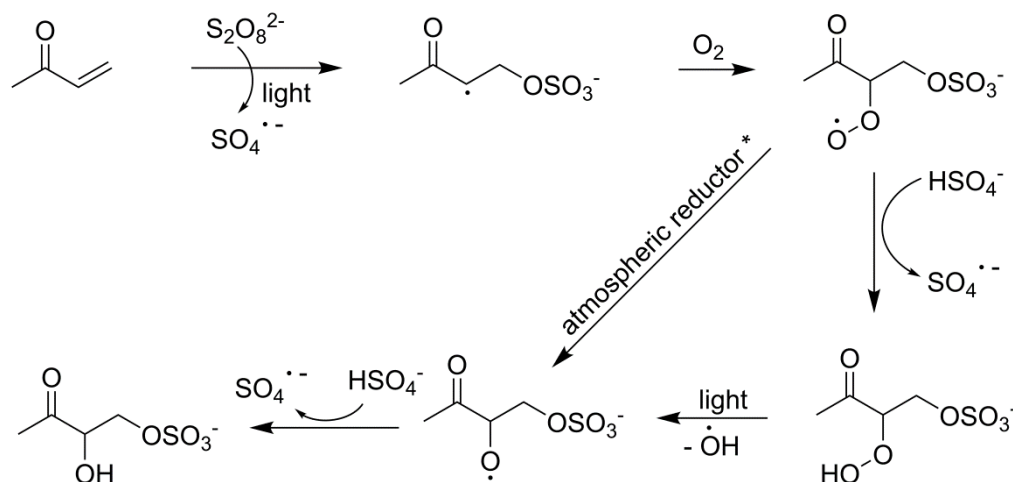
340

341 **Scheme 1.** Postulated fragmentation pathways of the MW 184 organosulfate originating from
 342 MVK aqueous : B1) early-eluting isomer with the retention time 0.92 min and B2) late-eluting
 343 isomer with the retention time of 0.96 min.

344

345 A possible reaction pathway for the formation of the MW184 organosulfate from MVK is
 346 presented in Scheme 2. Sulfate radicals that form by the homolytic dissociation of
 347 peroxydisulfate add to the C=C double bond of methyl vinyl ketone to form a distonic ion with
 348 negative charge located on the sulfate group and the radical on the carbon atom. Then, an
 349 oxygen molecule, dissolved in the aqueous solution adds to the radical center giving rise to a
 350 peroxy radical. In a further reaction, the latter abstracts a hydrogen atom from a bisulfate ion,
 351 which is ubiquitous in experimental solutions and turns into the hydroperoxide. Under solar
 352 light irradiation, hydroperoxide can dissociate into OH and alkoxy radical, which then can
 353 abstract hydrogen from bisulfate anion and turn into the MW 184 product. On the other hand,
 354 in atmospheric waters a peroxy \rightarrow alkoxy radical transition can be pursued by other

355 dissolved species, such as ubiquitous S(IV) species, e.g., sulfite anions (Townsend et al.,
 356 2012); however, the issue would require further laboratory studies.



357 m/z 183 OS

358

359 **Scheme 2.** A tentative reaction mechanism explaining the formation of the MW 184
 360 organosulfate from aqueous of MVK. (* Any atmospherically-relevant red-ox system, e.g.,
 361 $\text{HSO}_3^-/\text{SO}_3^{2-} \rightarrow \text{HSO}_4^-/\text{SO}_4^{2-}$)

362

363 *MW 200 organosulfate*

364

365 The MW 200 organosulfate originating from the aqueous-phase oxidation of MVK reveals an
 366 abundant product at the retention time of 0.83 min ($\text{C}_4\text{H}_7\text{O}_7\text{S}$; measured mass: 198.9901;
 367 error: -1.1 mDa), although neither the retention time nor the product ion spectrum are
 368 reflected in the MW 200 trace component of ambient $\text{PM}_{2.5}$ aerosol (Fig. 2 C, D). The
 369 presence of a MW 200 organosulfate originating from MVK in ambient fine aerosol was
 370 reported earlier (Schindelka et al., 2013); however, our results do not support the latter
 371 conclusion.

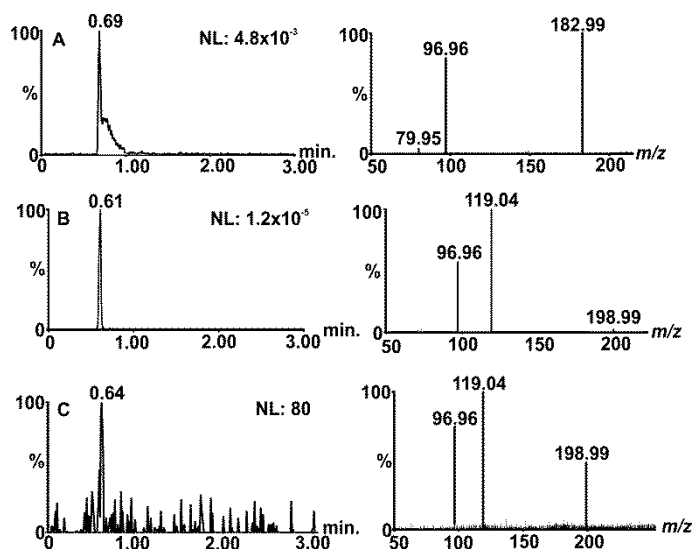
372

373 *3.5. Chemical characterization of products from aqueous of MACR*

374

375 The chemical characterization of MACR oxidation was targeted to C₃-C₄ organosulfates with
 376 the main detected products are listed in Table 1. The MW 154 organosulfate bears the same
 377 structural signature as that previously described for MVK.

378



379

380 **Fig. 3.** Extracted ion chromatograms and product ion spectra of: A) *m/z* 183 ion obtained
 381 through aqueous of MACR; B) *m/z* 199 in ambient PM_{2.5} aerosol; C) *m/z* 199 obtained
 382 through aqueous of MACR.

383

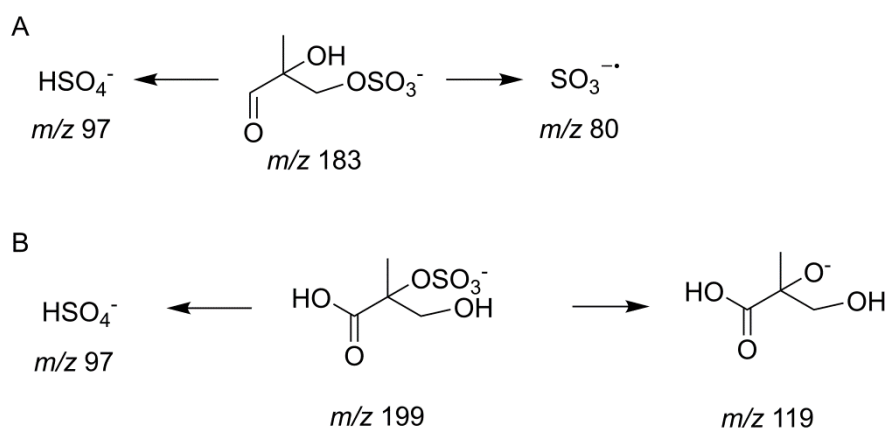
384 *MW 184 organosulfate*

385

386 The aqueous-phase reaction of MACR with the sulfate radicals leads to the formation of a
 387 MW 184 organosulfate (Fig. 3 A). In contrast to MVK, the MACR-derived organosulfate with
 388 the MW 184 was previously observed in ambient PM_{2.5} aerosol (e.g., Schindelka et al.,
 389 2013). Taking into consideration the fragmentation properties, it can be assumed that the
 390 position of the sulfate group is terminal since no characteristic neutral loss of formaldehyde
 391 (30 Da) is observed. The proposed fragmentation pathways are presented in Scheme 3 A.

392

393



394

395 **Scheme 3.** Proposed fragmentation channels for MACR-derived organosulfates A) the MW
396 184 and B) the MW 200 formed via aqueous reactions.

397

398 *MW 200 organosulfate*

399

400 The MW 200 organosulfate has been reported in previous laboratory experiments (Nozière et
401 al., 2010; Schindelka et al., 2013). The analysis of ambient PM_{2.5} aerosol reveals the MW
402 200 organosulfate as a single peak (C₄H₇O₇S; measured mass 198.9915, error: 0.3 mDa)
403 eluting at RT 0.61 min (Fig. 3 B). The aqueous-phase reaction gives rise to the MACR-
404 derived organosulfate featuring a similar retention time (RT. 0.64 min) and an identical
405 fragmentation profile (C₄H₇O₇S; measured mass 198.9927; error: 1.5 mDa) as that detected
406 in ambient PM_{2.5} aerosol (Fig. 3 B, C). A detailed analysis of the extracted ion chromatogram
407 (*m/z* 199) at a void time region along with the product ion spectrum led us to postulate a
408 structure bearing a carboxylic acid moiety, a hydroxymethyl moiety and sulfate group located
409 at the tertiary hydroxyl group. Although the fragmentation profile is not very informative (Fig.
410 3 B, C) we can conclude that an easy formation of the bisulfate ion at *m/z* 97 (HSO₄⁻)
411 requires access to the proton at the vicinal carbon atom (Scheme 3 B). If the sulfate group
412 was located at the terminal carbon, this fragmentation route would be less likely to occur
413 (Attygalle et al., 2001). As in case of the MVK-related MW184 OS differences are observed
414 for the retention times between the ambient PM_{2.5} sample and the aqSOA sample. In the

415 PM_{2.5} sample the peak elutes slightly earlier, which most probably indicates different matrix
416 comparing to aqSOA from laboratory experiment.

417

418 4. Conclusions

419

420 We showed that two atmospherically relevant α , β -unsaturated carbonyls, but-3-en-2-on
421 (methyl vinyl ketone, MVK) and prop-2-en-1-on (methacrolein, MACR)
422 undergo transformations induced by sulfate radicals in dilute aqueous systems under solar
423 irradiation to form the organosulfates that were previously identified in ambient aerosols and
424 in smog chamber-generated SOA. A detailed interpretation of negative ion electrospray mass
425 spectra along with accurate mass measurements allowed for the molecular characterization
426 of several organosulfates: MWs 154 (C₃H₅O₅S), 156 (C₂H₃O₆S), 168 (C₄H₇O₅S), 184
427 (C₄H₇O₆S) and 200 (C₄H₇O₇S) that were products of MVK oxidation; and MWs 154
428 (C₃H₅O₅S), 184 (C₄H₇O₆S) and 200 (C₄H₇O₇S) that were products of MACR oxidation. The
429 interpretation of MS² mass spectra recorded for MVK-derived organosulfate (MW 184) let us
430 revise its molecular structure. Kinetic analysis based on UV-spectra showed that both MACR
431 and MVK oxidations were fast processes. Therefore, we suggest that photooxidation of
432 MACR and MVK induced by radicals can likely take place in atmospheric waters and lead to
433 formation of aqSOA. Atmospheric waters, which take the form of clouds, rain, fog and dew,
434 offer an ubiquitous environment hosting radical precursors such as SO₂ and H₂O₂. Irradiated
435 by sun, they become a chemical reactor potentially capable of transforming atmosphere
436 organic components into oxidized and functionalized products that contribute to the aqSOA
437 formation. Revealing the molecular identity and structure of these products, and the
438 mechanisms of their formation enables the construction of more accurate models for
439 predicting SOA formation in the atmosphere and its implication on climate change. A recent
440 modelling study showed that aqueous-phase processes can likely contribute to 20-30 Tg
441 year⁻¹ production of aqSOA, which is a substantial fraction in the still underestimated budget
442 of atmospheric aerosol (McNeill, 2015). On the other hand, detailed understanding of the

443 SOA composition helps to track and eventually reduce or eliminate the sources of SOA
444 precursors. Atmospheric transformation of MACR and MVK into aqueous organosulfates is
445 expected in regions with considerable emission of isoprene such as deciduous woodlands or
446 rain forests. The indispensable precursors of sulfate radicals include natural and
447 anthropogenic sulfur dioxide and, according to some researchers (e.g., Nozière et al., 2010),
448 inorganic sulfates, which are ubiquitous components of atmospheric aerosol.

449

450

451 **Acknowledgments**

452

453 The research was partially supported by the funding from the Polish National Science Centre
454 (grant Nr OPUS8-2014/15/B/ST10/04276).

455 **References**

456
457 Attygalle, A.B., Garcia-Rubio, S., Ta, J., Meinwald, J., 2001. Collisionally-induced
458 dissociation mass spectra of organic sulfate anions. *J. Chem. Soc. Perkin Trans. 2.* 498-506.

459
460 Bianchi, F., Tröstl, J., Junninen, H., Frege, C., Henne, S., Hoyle, C.R., Molteni, U.,
461 Herrmann, E., Adamov, A., Bukowiecki, N., Chen, X., Duplissy, J., Gysel, M., Hutterli, M.,
462 Kangasluoma, J., Kontkanen, J., Kürten, A., Manninen, H. E., Münch, S., Peräkylä, O.,
463 Petäjä, T., Rondo, L., Williamson, C., Weingartner, E., Curtius, J., Worsnop, D. R., Kulmala,
464 M., Dommen, J., Baltensperger, U., 2016. New particle formation in the free troposphere: A
465 question of chemistry and timing. *Science* 352, 1109-1112.

466
467 Blando, J.D., Turpin, B.J., 2000. Secondary organic aerosol formation in cloud and fog
468 droplets: a literature evaluation of plausibility. *Atmos. Environ.* 34, 1623-1632.

469
470 von Sonntag, C.S., Schuchmann, H. P., 1991. The elucidation of peroxy radical reactions in
471 aqueous solution with the help of radiation-chemical methods. *Angew. Chem., Int. Ed. Engl.*
472 30, 1229-1253.

473
474 Carlton, A.G., Wiedinmyer, C., Kroll, J. H., 2009. A review of Secondary Organic Aerosol
475 (SOA) formation from isoprene. *Atmos. Chem. Phys.* 9, 4987-5005.

476
477 Claeys, M., Bim, G., Vas, G., Wang, W., Vermeylen, R., Pashynska, V., Cafmeyer, J.,
478 Guyon, P., Andreae, M. O., Artaxo, P., Maenhaut, W., 2004. Formation of Secondary
479 Organic Aerosols through photooxidation of isoprene. *Science* 303, 1173-1176.

480

- 481 Darer, A.I., Cole-Filipiak, N. C., O'Connor, A. E., Elrod, M. J., 2011. Formation and stability of
482 atmospherically relevant isoprene-derived organosulfates and organonitrates. *Environ. Sci.*
483 *Technol.* 45, 1895-1902.
- 484
- 485 Ervens, B., Turpin, B. J., Weber, R. J., 2011. Secondary organic aerosol formation in cloud
486 droplets and aqueous particles (aqSOA): a review of laboratory, field and model studies.
487 *Atmos. Chem. Phys.* 11, 11069-11102.
- 488
- 489 Giorio, C., Monod, A., Bregonzio-Rozier, L., DeWitt, H. L., Cazaunau, M., Temime-Roussel,
490 B., Gratien, A., Michoud, V., Pangu, E., Ravier, S., Zielinski, A. T., Tapparo, A., Vermeylen,
491 R., Claeys, M., Voisin, D., Kalberer, M., Doussin, J.-F., 2017. Cloud processing of Secondary
492 Organic Aerosol from isoprene and methacrolein photooxidation. *J. Phys. Chem. A.* 121,
493 7641–7654.
- 494
- 495 Hallquist, M., Wenger, J. C., Baltensperger, U., Rudich, Y., Simpson, D., Claeys, M.,
496 Dommen, J., Donahue, N. M., George, C., Goldstein, A. H., Hamilton, J. F., Herrmann, H.,
497 Hoffmann, T., Iinuma, Y., Jang, M., Jenkin, M. E., Jimenez, J. L., Kiendler-Scharr, A.,
498 Maenhaut, W., McFiggans, G., Mentel, Th F., Monod, A., Prévôt, A. S. H., Seinfeld, J. H.,
499 Surratt, J. D., Szmigielski, R., Wildt, J., 2009. The formation, properties and impact of
500 secondary organic aerosol: current and emerging issues. *Atmos. Chem. Phys.* 9, 5155-5236.
- 501
- 502 Hansen, A.M.K., Kristensen, K., Nguyen, Q. T., Zare, A., Cozzi, F., Nøjgaard, J. K., Skov, H.,
503 Brandt, J., Christensen, J. H., Ström, J., Tunved, P., Krejci, R., Glasius, M., 2014.
504 Organosulfates and organic acids in Arctic aerosols: speciation, annual variation and
505 concentration levels. *Atmos. Chem. Phys.* 14, 7807-7823.
- 506
- 507 Herrmann, H., Schaefer, T., Tilgner, A., Styler, S. A., Weller, C., Teich, M., Otto, T., 2015.
508 Tropospheric aqueous-phase chemistry: kinetics, mechanisms, and its coupling to a
509 changing gas phase. *Chem. Rev.* 115, 4259-4334.
- 510
- 511 Kameel, F.R., Riboni, F., Hoffmann, M. R., Enami, S., Colussi, A. J., 2014. Fenton oxidation
512 of gaseous isoprene on aqueous surfaces. *J. Phys. Chem. C.* 118, 29151-29158.
- 513
- 514 Kolthoff, I.M.; Miller, I.K., 1951. The chemistry of persulfate. I. The kinetics and mechanism of
515 the decomposition of the persulfate ion in aqueous medium. *J. Am. Chem. Soc.* 73, 3055-
516 3059.
- 517
- 518 Kwong, K.C., Chim, M. M., Davies, J. F., Wilson, K. R., Chan, M. N., 2018. Importance of
519 sulfate radical anion formation and chemistry in heterogeneous OH oxidation of sodium
520 methyl sulfate, the smallest organosulfate. *Atmos. Chem. Phys.* 18, 2809-2820.
- 521
- 522 Leng, C., Kish, J. D., Kelley, J., Mach, M., Hiltner, J., Zhang, Y., Liu, Y., 2013. Temperature-
523 dependent Henry's Law constants of atmospheric organics of biogenic origin. *J. Phys. Chem.*
524 *A.* 117, 10359-10367.
- 525
- 526 Liang, C.S., Duan, F. K., He, K. B., Ma, Y. L., 2016. Review on recent progress in
527 observations, source identifications and countermeasures of PM_{2.5}. *Environ. Int.* 86, 150-
528 170.
- 529
- 530 Liu, Y., Monod, A., Tritscher, T., Praplan, A. P., DeCarlo, P. F., Temime-Roussel, B., Quivet,
531 E., Marchand, N., Dommen, J., Baltensperger, U., 2012. Aqueous phase processing of
532 secondary organic aerosol from isoprene photooxidation. *Atmos. Chem. Phys.* 12, 5879-
533 5895.
- 534

- 535 McNeill, V.F., 2015. Aqueous organic chemistry in the atmosphere: sources and chemical
536 processing of organic aerosols. *Environ. Sci. Technol.* 49, 1237-1244.
537
- 538 Monks, P.S., 2005. Gas-phase radical chemistry in the troposphere. *Chem. Soc. Rev.* 34,
539 376-395.
540
- 541 Nguyen, T.B., Coggon, M. M., Bates, K. H., Zhang, X., Schwantes, R. H., Schilling, K. A.,
542 Loza, C. L., Flagan, R. C., Wennberg, P. O., Seinfeld, J. H., 2014. Organic aerosol formation
543 from the reactive uptake of isoprene epoxydiols (IEPOX) onto non-acidified inorganic seeds.
544 *Atmos. Chem. Phys.* 14, 3497-3510.
545
- 546 Noziere, B., 2016. Don't forget the surface. *Science* 351, 1396-1397.
547
- 548 Nozière, B., Ekström, S., Alsberg, T., Holmström, S., 2010. Radical-initiated formation of
549 organosulfates and surfactants in atmospheric aerosols. *Geophys. Res. Lett.* 37, L05806,
550 doi:10.1029/2009GL041683.
551
- 552 Nozière, B., Kalberer, M., Claeys, M., Allan, J., D'Anna, B., Decesari, S., Finessi, E., Glasius,
553 M., Grgić, I., Hamilton, J. F., Hoffmann, T., Iinuma, Y., Jaoui, M., Kahnt, A., Kampf, C. J.,
554 Kourtchev, I., Maenhaut, W., Marsden, N., Saarikoski, S., Schnelle-Kreis, J., Surratt, J. D.,
555 Szidat, S., Szmigielski, R., Wisthaler, A., 2015. The molecular identification of organic
556 compounds in the atmosphere: state of the art and challenges. *Chem. Rev.* 115, 3919-3983.
557
- 558 Ouyang, B., Fang, H. J., Zhu, C. Z., Dong, W. B., Hou, H. Q., 2005. Reactions between the
559 SO₄ center dot-radical and some common anions in atmospheric aqueous droplets. *J.*
560 *Environ. Sci. China* 17, 786-788.
561
- 562 Renard, P., Siekmann, F., Salque, G., Demelas, C., Coulomb, B., Vassalo, L., Ravier, S.,
563 Temime-Roussel, B., Voisin, D., Monod, A., 2015. Aqueous-phase oligomerization of methyl
564 vinyl ketone through photooxidation - Part 1: Aging processes of oligomers. *Atmos. Chem.*
565 *Phys.* 15, 21-35.
566
- 567 Rudzinski, K.J., 2004. Degradation of isoprene in the presence of sulphy radical anions. *J.*
568 *Atmos. Chem.* 48, 191-216.
569
- 570 Rudziński, K.J., Gmachowski, L., Kuznietsova, I., 2009. Reactions of isoprene and sulphy
571 radical-anions – a possible source of atmospheric organosulphites and organosulphates.
572 *Atmos. Chem. Phys.* 9, 2129-2140.
573
- 574 Rudzinski, K.J., Szmigielski, R., Kuznietsova, I., Wach, P., Staszek, D., 2016. Aqueous-
575 phase story of isoprene - A mini-review and reaction with HONO. *Atmos. Environ.* 130, 163-
576 171.
577
- 578 Safi Shalamzari, M., Ryabtsova, O., Kahnt, A., Vermeylen, R., Hérent, M.-F., Quetin-
579 Leclercq, J., Van der Veken, P., Maenhaut, W., Claeys, M., 2013. Mass spectrometric
580 characterization of organosulfates related to secondary organic aerosol from isoprene. *Rapid*
581 *Comm. Mass Spectrom.* 27, 784-794.
582
- 583 Schindelka, J., Iinuma, Y., Hoffmann, D., Herrmann, H., 2013. Sulfate radical-initiated
584 formation of isoprene-derived organosulfates in atmospheric aerosols. *Faraday Discuss.* 165,
585 237-259.
586
- 587 Schöne, L., Herrmann, H., 2014. Kinetic measurements of the reactivity of hydrogen
588 peroxide and ozone towards small atmospherically relevant aldehydes, ketones and organic
589 acids in aqueous solutions. *Atmos. Chem. Phys.* 14, 4503-4514.

- 590
591 Schöne, L., Schindelka, J., Szeremeta, E., Schaefer, T., Hoffmann, D., Rudzinski, K. J.,
592 Szmigielski, R., Herrmann, H., 2014. Atmospheric aqueous phase radical chemistry of the
593 isoprene oxidation products methacrolein, methyl vinyl ketone, methacrylic acid and acrylic
594 acid -kinetics and product studies. *Phys. Chem. Chem. Phys.* 16, 6257-6272.
595
- 596 Shalamzari, M.S., Vermeylen, R., Blockhuys, F., Kleindienst, T. E., Lewandowski, M.,
597 Szmigielski, R., Rudzinski, K. J., Spólnik, G., Danikiewicz, W., Maenhaut, W., Claeys, M.,
598 2016. Characterization of polar organosulfates in secondary organic aerosol from the
599 unsaturated aldehydes 2-E-pentenal, 2-E-hexenal, and 3-Z-hexenal. *Atmos. Chem. Phys.*
600 16, 7135-7148.
601
- 602 Sindelarova, K., Granier, C., Bouarar, I., Guenther, A., Tilmes, S., Stavrakou, T., Muller, J.
603 F., Kuhn, U., Stefani, P., Knorr, W., 2014. Global data set of biogenic VOC emissions
604 calculated by the MEGAN model over the last 30 years. *Atmos. Chem. Phys.* 14, 9317-
605 9341.
606
- 607 Spólnik, G., Wach, P., Rudzinski, K. J., Skotak, K., Danikiewicz, W., Szmigielski, R., 2018.
608 Improved UHPLC-MS/MS methods for analysis of isoprene-derived organosulfates. *Anal.*
609 *Chem.* 90, 3416-3423.
610
- 611 Surratt, J.D., Murphy, S. M., Kroll, J. H., Ng, N. L., Hildebrandt, L., Sorooshian, A.,
612 Szmigielski, R., Vermeylen, R., Maenhaut, W., Claeys, M., Flagan, R. C., Seinfeld, J. H.,
613 2006. Chemical composition of secondary organic aerosol formed from the photooxidation of
614 isoprene. *J. Phys. Chem. A.* 110, 9665-9690.
615
- 616 Surratt, J.D., Kroll, J. H., Kleindienst, T. E., Edney, E. O., Claeys, M., Sorooshian, A., Ng, N.
617 L., Offenberg, J. H., Lewandowski, M., Jaoui, M., Flagan, R. C., Seinfeld, J. H., 2007.
618 Evidence for organosulfates in secondary organic aerosol. *Environ. Sci. Technol.* 41, 517-
619 527.
620
- 621 Szmigielski, R., 2016. Evidence for C₅ organosulfur secondary organic aerosol components
622 from in-cloud processing of isoprene: Role of reactive SO₄ and SO₃ radicals. *Atmos. Environ.*
623 130, 14-22.
624
- 625 Szmigielski, R., Surratt, J. D., Vermeylen, R., Szmigielska, K., Kroll, J. H., Ng, N. L., Murphy,
626 S. M., Sorooshian, A., Seinfeld, J. H., Claeys, M., 2007. Characterization of 2-methylglyceric
627 acid oligomers in secondary organic aerosol formed from the photooxidation of isoprene
628 using trimethylsilylation and gas chromatography/ion trap mass spectrometry. *J. Mass*
629 *Spectrom.* 42, 101-116.
630
- 631 Townsend, T.M., Allanic, A., Noonan, C., Sodeau, J. R., 2012. Characterization of sulfurous
632 acid, sulfite, and bisulfite aerosol systems. *J. Phys. Chem. A.* 116, 4035-4046.
633
- 634 van Pinxteren, D., Plewka, A., Hofmann, D., Mueller, K., Kramberger, H., Svrčina, B.,
635 Baechmann, K., Jaeschke, W., Mertes, S., Collett, J. L., Herrmann, H. 2005. Schmucke hill
636 cap cloud and valley stations aerosol characterisation during FEBUKO (II): Organic
637 compounds. *Atmos. Environ.*, 39, 4305-4320.
638
- 639 Zhao, H., Jiang, X., Du, L., 2017. Contribution of methane sulfonic acid to new particle
640 formation in the atmosphere. *Chemosphere* 174, 689-699.

Highlights

- Methacrolein and methyl vinyl ketone form SOA in atmospheric waters
- This proceeds through SO_4 radical-mediated reactions to form organosulfates
- Structures of organosulfates formed were elucidated and in some cases revised
- An abundant isoprene-related organosulfate $\text{C}_4\text{H}_8\text{SO}_7$ (m/z 199) was detected
- Sunlight enhances the oxidative capacity of atmospheric waters